Hyperfine Interact (2016) 237: 142
DOI 10.1007/s10751-016-1358-6

Progress of the nEDM experiment at the Paul Scherrer Institute

Małgorzata Kasprzak[1]

Published online: 5 October 2016

Abstract Advances in experimental searches for a neutron Electric Dipole Moment (nEDM,d_n) are motivated by the potential discovery of a new source of CP violation beyond the Standard Model of particle physics. The nEDM experiment at the Paul Scherrer Institute (PSI), which with accumulated sensitivity of 1.09×10^{-26} e·cm (September 2016) is currently the most sensitive nEDM experiment worldwide, uses the Ramsey technique of separated oscillatory fields applied to stored ultracold neutrons. The nEDM measurements depend upon precise information about the magnetic field, which is monitored by a ^{199}Hg co-magnetometer and an array of ^{133}Cs magnetometers. The principle of the magnetic field measurement is based on the optical detection of the Larmor precession frequency of atoms polarized by optical pumping. In this article we present the recent progress of the nEDM experiment as well as details of a magnetic field measurements with special focus on the laser-operated array of high-sensitivity ^{133}Cs magnetometers.

Keywords Neutron electric dipole moment · CP invariance · Magnetometery · Ultracold neutrons

1 Introduction

The inconsistency between the observed baryon asymmetry of the Universe (expressed as a ratio η of number of baryons n_b to number of photons n_γ), $\eta = n_b/n_\gamma = 6.05 \times 10^{-10}$ [1] and the predictions of cosmological models leading to $\eta = 10^{-18}$ [2], implies that in the

On behalf of the nEDM collaboration http://nedm.web.psi.ch.

This article is part of the Topical Collection on *Proceedings of the International Conference on Hyperfine Interactions and their Applications (HYPERFINE 2016), Leuven, Belgium, 3-8 July 2016.*

✉ M. Kasprzak
malgorzata.kasprzak@fys.kuleuven.be

1 Institute for Nuclear and Radiation Physics, University of Leuven, 3001 Leuven, Belgium

early stage of the Universe the laws of physics for matter and for antimatter were different. This indicates that CP symmetry, i.e. the combined charge conjugation C and parity P symmetry of the fundamental interactions, was not conserved [3]. The Standard Model (SM) theory of particle physics, based on the experimental evidence of CP violation in neutral kaon [4] and B-meson [5, 6] systems, includes a CP-violating parameter in electroweak interactions, but this cannot account for the observed matter-antimatter asymmetry. This has triggered the development of various theoretical models incorporating sources of CP violation beyond the SM. On the experimental side, the ongoing research on CP violation is divided into the following branches: (i) searches for CP-violating phenomena in high-energy particle physics experiments [7], (ii) searches for CP-violation in neutrino oscillations [8] and (iii) searches for CP-violating permanent electric dipole moments of electron, neutron and neutral atoms [9]. The main focus of interest in this article is one of the latter experiments, namely an experiment searching for the electric dipole moment of a neutron (nEDM).

The Hamiltonian describing the interaction of an electric field **E** with an nEDM (d_n) projected onto the neutron's spin $\boldsymbol{\sigma}$, $H_E = d_n \frac{\boldsymbol{\sigma}}{|\boldsymbol{\sigma}|} \cdot \mathbf{E}$, is T (time reversal) and P (parity) odd, and assuming the validity of the CPT theorem [10], which states that any system must remain unchanged under the combined C, P, T operations, it also violates CP symmetry. The SM prediction for nEDM, taking into account the CP-violating parameter δ, gives a value of about 10^{-32} e·cm [11], which is several orders of magnitude lower than the current nEDM limit of 3×10^{-26} e·cm [12] and beyond reach of any foreseen experimental efforts. On the other hand, most of the New Physics scenarios predict nEDM values larger than 10^{-28} e·cm [13], which could be detected in current and/or near-future experiments.

2 Principle of nEDM measurement

The concept of the nEDM measurement is based on a precise determination of neutron's spin precession frequency ν_{prec} in the magnetic **B** and electric **E** fields aligned either parallel ($\xi = \hat{E} \cdot \hat{B} = +1$) or anti-parallel ($\xi = -1$) to each other. The neutron interacts with the magnetic field via the magnetic moment μ_n, and its Larmor precession frequency ν_L is given by

$$\nu_L = \frac{\gamma_n}{2\pi}|\mathbf{B}| = \frac{2\mu_n|\mathbf{B}|}{h} \tag{1}$$

where γ_n=$2\pi \times 29.1646933(69)$ MHz/T [14] is the gyromagnetic ratio of the neutron. The interaction of the electric dipole moment of the neutron with an electric field can be expressed in analogy to Eq. 1, leading ultimately to

$$h\nu_\xi = h(\nu_L + \xi\nu_E) = 2\mu_n|\mathbf{B}| + \xi 2d_n|\mathbf{E}|. \tag{2}$$

Any difference in the precession frequency between measurements with the electric field parallel (ν_+) and anti-parallel (ν_-) to the magnetic field indicates the presence of the nEDM:

$$d_n = \frac{h}{4|\boldsymbol{E}|}(\nu_+ - \nu_-). \tag{3}$$

Equation 3 assumes that the magnetic field in both field configurations remains exactly the same, whereas in reality this condition is impossible to achieve. The $dn = (n_+ - n_-)$ of order 10^{-26} e·cm corresponds to a frequency difference $\delta\nu = (\upsilon_+ - \upsilon_-)$ of about 1.1×10^{-7} Hz, which translates to a magnetic field difference of $\delta B = \delta\nu/\gamma_n/2\pi = 4 \times 10^{-15}$T, which is a factor 10^{10} smaller than the Earth's magnetic field. Hence, precise magnetic field control

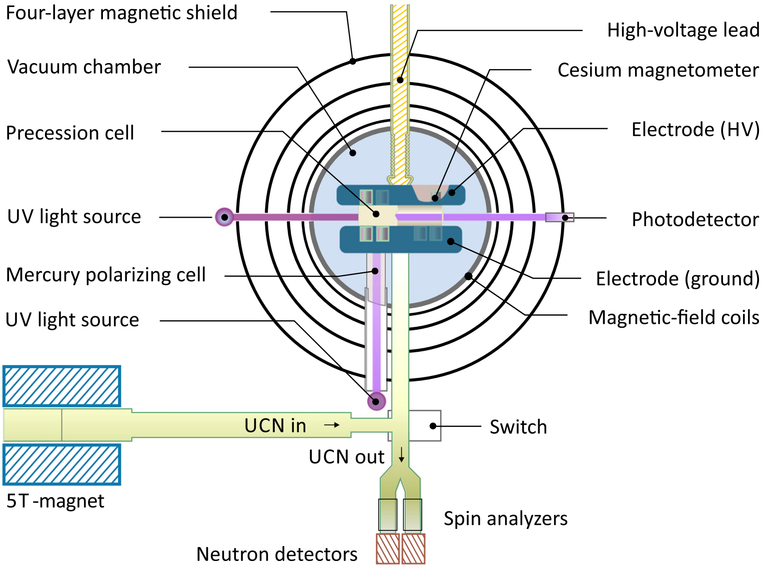

Fig. 1 The scheme of the nEDM apparatus at PSI (upgraded version of RAL/Sussex/ILL setup[18])

and monitoring is one of the biggest challenges of all nEDM experiments. Measurements are therefore performed in a magnetically shielded environment [15] suppressing the effects of external field fluctuations. The magnetic field **B** inside the magnetic shield is monitored with high-sensitivity ^{199}Hg and ^{133}Cs magnetometers (Section 4)

3 Experimental technique

The nEDM experiment [16] located at the Paul Scherrer Institute (PSI) is performed using ultracold neutrons (UCN) from the PSI UCN source [17], which are guided to the experiment, trapped in the precession chamber and exposed to **E** (11 kV/cm) and **B** (1 μT) fields. The experimental components are shown in Fig. 1. The advantage of using UCN, i.e. neutrons with very low kinetic energies (typically $E_k < 3 \times 10^{-7}$eV) is the ability to store UCN in a trap for hundreds of seconds, thereby increasing the sensitivity of the measurements and greatly suppressing systematic effects of motional $\mathbf{v} \times \mathbf{E}$ related magnetic fields.

The UCN are spin-polarized by transmission through the 5 T magnetic field, and are guided to the precession chamber where they are stored and exposed to the ambient **B** and **E** fields. Following the Ramsey cycle (see Section 3.1) the UCN are spin analysed and counted in a dedicated neutron detection system [19, 20].

The systematic effects related to the magnetic field are controlled by the ^{199}Hg co-magnetometer, which fills the precession chamber together with UCN, and the laser driven array of ^{133}Cs magnetometers. The ^{199}Hg co-magnetometer atoms are spin-polarized in the mercury polarizing cell (Fig. 1) and fill the precession chamber together with UCN during the Ramsey cycle. Following the $\pi/2$ spin flip of frequency corresponding to the Larmor frequency of ^{199}Hg, the ^{199}Hg atoms precess around the magnetic field **B**. The spin-precession of ^{199}Hg atoms is read by the circularly polarized light from the ^{204}Hg discharge lamp of a

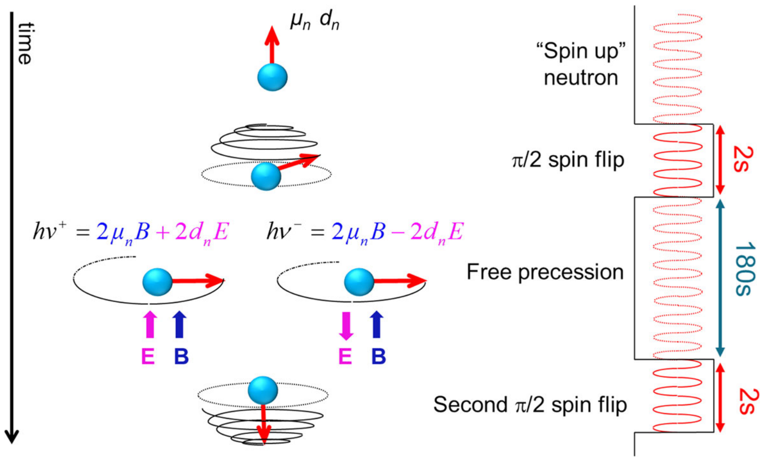

Fig. 2 A cartoon illustrating the principle of a single measurement, based on Fig. 4 of [22]

wavelength of 253.7 nm and recorded on the photmultiplier. The spin-precession frequency of ^{199}Hg is used to correct for magnetic field drifts during the Ramsey cycle. The array of sixteen ^{133}Cs magnetometers (Section 4.1) located below and above the precession chamber measures the spatial distribution of the magnetic field allowing improvements of field homogeneity and extraction of the gradient $\partial B_z/\partial z$ along the neutron precession chamber.

3.1 Ramsey method

The neutrons' precession frequency is determined by the Ramsey technique [21] of separated oscillatory fields, as illustrated in Fig. 2. The spins of polarized neutrons trapped in the precession chamber are flipped by a 2 s long pulse of frequency ν_{rf} and then precess freely with $\nu_+, \nu_- \sim 30$ Hz about the **B** and **E** fields for a time T = 180 s. If the applied pulses are precisely on resonance, the second spin flip (coherent with the first) sets the final neutron polarization to the state opposite to the initial one. The spin-sensitive detection of UCN allows extraction of an asymmetry value A for a single frequency measurement, $A = (N^{\uparrow} - N^{\downarrow})/(N^{\uparrow} + N^{\downarrow})$), where N is the number of counted UCN and the arrows indicate the spin direction. The data are taken at off-resonance frequencies, at four working points: two at each side of the resonant frequency (Fig. 3). The asymmetry is shown as a function of the ratio $R = \nu_{rf}/\nu_{Hg}$, where ν_{Hg} is the measured precession frequency of cohabiting ^{199}Hg atoms, in order to correct for unavoidable magnetic field changes. The ratio R_a at the neutron resonance frequency is determined from the fit function

$$A = A_{av} - \alpha \cos\left(\frac{\pi \langle \nu_{Hg} \rangle}{\Delta\nu}(R - R_a)\right), \tag{4}$$

where $\alpha = (A_{max} - A_{min})/(A_{max} + A_{min})$ and $\langle \nu_{Hg} \rangle$ is the average ^{199}Hg frequency. The statistical sensitivity of one Ramsey cycle is

$$\delta(d_n) = \frac{\hbar}{2\alpha T E\sqrt{N}}, \tag{5}$$

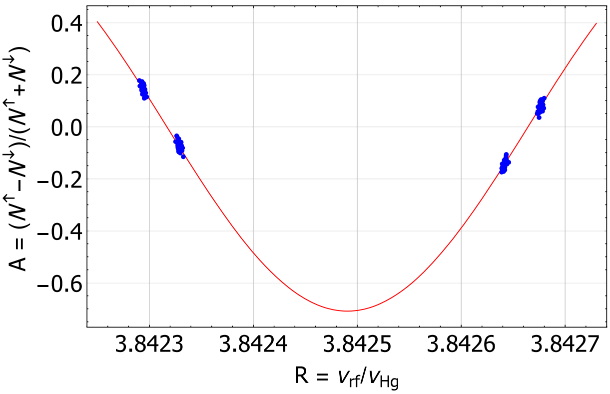

Fig. 3 The central Ramsey fringe: The neutron asymmetry data as a function of $R = \nu_{rf}/\nu_{Hg}$ for one **E**, **B** field configuration. Each data point represents the result from a single Ramsey sequence as shown in Fig. 2. The line represents the fit to the data according to Eq. 4. The data are taken at four working points, i.e. at four ν_{rf} frequencies, each slightly detuned from the resonant frequency. The ν_{rf} frequencies are divided by the precession frequency of ^{199}Hg, ν_{Hg}, in order to correct for the magnetic field fluctuations

where T is the precession time, E the electric field strength and N the number of detected neutrons. In the last two years of data taking there have been in total about 35000 Ramsey cycles performed with an average statistical sensitivity (Eq. 5) per cycle of $2.3 \times 10^{-24} e\cdot$cm. Based on this, an upper limit on the magnetometer sensitivity can be estimated, leading to $\delta B < 400 fT$ in a single measurement.

4 Magnetic field control and monitoring

Effects related to magnetic field changes and inhomogeneities provide the dominant systematic errors in the nEDM experiment at PSI. A detailed description of these systematic effects is given in [12]. The magnetic field **B**, oriented along the longitudinal axis z of the precession chamber, is created by the cos-theta coil. The homogeneous distribution of the field is additionally improved by applying small currents to the 33 correcting coils. The magnetic-field changes are monitored by two magnetometry sytems; a ^{199}Hg co-magnetometer [23], and the array of sixteen ^{133}Cs magnetometers [24, 25]. During the Ramsey cycle the spin-polarized ^{199}Hg atoms fill the precession chamber together with the neutrons, and their precession frequency ν_{Hg} is recorded to give a direct measure of the magnetic field during this cycle, according to $\nu_{Hg} = \gamma_{Hg}|\mathbf{B}|$ where $\gamma_{Hg} = 7.590118(13)$ MHz/T [26]. The ^{199}Hg frequency is used to correct the neutron resonance frequency ν_n for the magnetic field changes during the cycle [18]. The drawback of this method is that there is a difference (Δh) between the centers of gravity of UCN and ^{199}Hg, as the ^{199}Hg probe the whole volume while the UCN preferentially occupy the lower part of the precession chamber due to their low energies. Asa consequence, the ratio R_a depends on the magnetic field gradient $\partial B_z/\partial z$ across the precession chamber [27]:

$$R_a = \frac{\nu_n}{\nu_{Hg}} = \frac{\gamma_n}{\gamma_{Hg}} \left(1 \pm \Delta h \frac{\partial B_z/\partial z}{|\mathbf{B}|}\right) \tag{6}$$

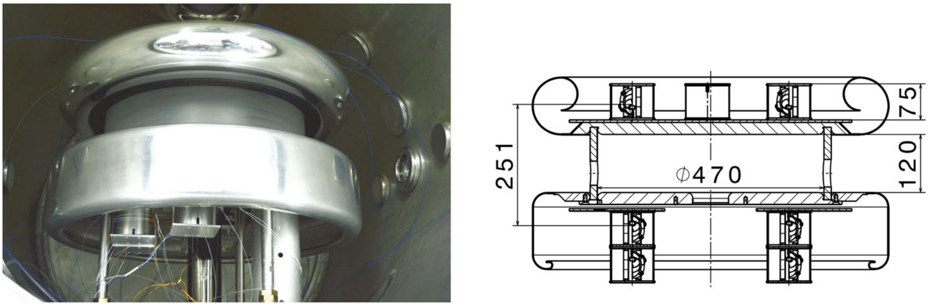

(a) (b)

Fig. 4 **a** Picture of the inside of the vacuum chamber of the experiment, showing the precession chamber and the two electrodes (HV and ground and the corona rings). Below the bottom electrode a few ^{133}Cs magnetometers (inside cylindrical aluminium covers) are visible. **b** Section drawing of the nEDM precession chamber and electrodes with ^{133}Cs sensors

where the sign is determined by the sense of the magnetic field **B** which can be oriented either up ($\mathbf{B}_{up}$) or down ($\mathbf{B}_{down}$) along the z-axis direction. In order to correct for this effect[1] the d_n value is obtained by a so-called crossing-point analysis [12] and the measurements are performed at various magnetic field gradients $\partial B_z/\partial z$ ranging from about -40 to 40 pT/cm for two magnetic field directions, $\mathbf{B}_{up}$ and $\mathbf{B}_{down}$. Each $\partial B_z/\partial z$ gradient configuration is carefully prepared and characterized with the help of an array of ^{133}Cs magnetometers located above and below the neutrons' precession chamber (Fig. 4). The nEDM measurements in one magnetic field configuration typically take a few days, resulting in about 400 Ramsey cycles within one run.

4.1 Operation principle of ^{133}Cs sensors

The ^{133}Cs magnetometers measure the Larmor frequency of ^{133}Cs atoms, $\nu_{Cs} = \gamma_{Cs}|\mathbf{B}|$ with $\gamma_{Cs} = 3498.62110(36)$ MHz/T [29] using optical detection of the magnetic resonance of ^{133}Cs atoms in a static magnetic field **B**. The ^{133}Cs magnetometer (Fig. 5) consists of a paraffine-coated glass cell filled with ^{133}Cs vapour at room temperature [30]. Infrared laser light of wavelength 894 nm passes though the ^{133}Cs cell, which lies within the rf coils, and is then detected by the photodiode. Circularly polarized laser light resonant with the F = 4 → F' = 3 hyperfine transition, initially polarizes the atoms by transferring them from the absorbing 'bright' sublevels into the non-absorbing 'dark' states. The coherent transitions between the 'bright' and 'dark' Zeeman sublevels are resonantly driven by an oscillating magnetic field B_{rf} with frequency $\nu_{rf} = \nu_{Cs}$ produced by the rf coils (Fig. 5a).The intensity of the laser light passing through the ensemble of ^{133}Cs atoms is modulated at the frequency corresponding to ν_{Cs}, due to the change of the absorption coefficient. This signal is detected on a photodiode and analysed by a lock-in demodulation technique. The continuous operation of the sensor is ensured by a feedback loop algorithm that keeps the $\nu_{rf} = \nu_{Cs}$. A dedicated DAQ system provides magnitude of the magnetic field $|\mathbf{B}|$ for each ^{133}Cs magnetometer, with a 1 kHz sampling rate.

[1] Other systematic effects related to the magnetic field gradient are described in detail in Ref. [12] and [28]

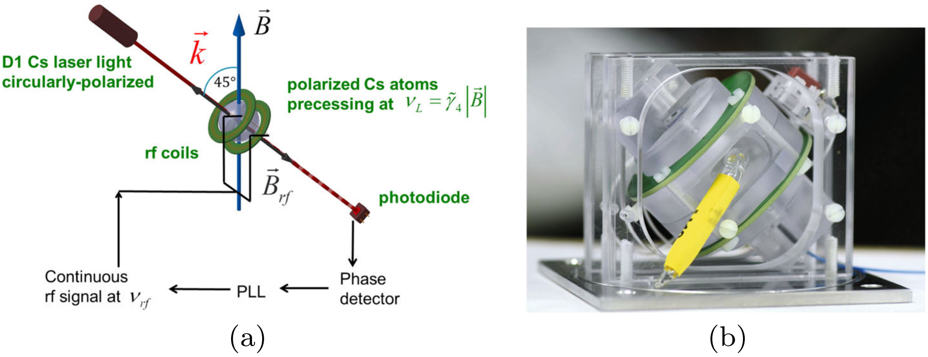

Fig. 5 **a** Principle of the ^{133}Cs sensor operation. **b** Picture of the assembled ^{133}Cs magnetometer

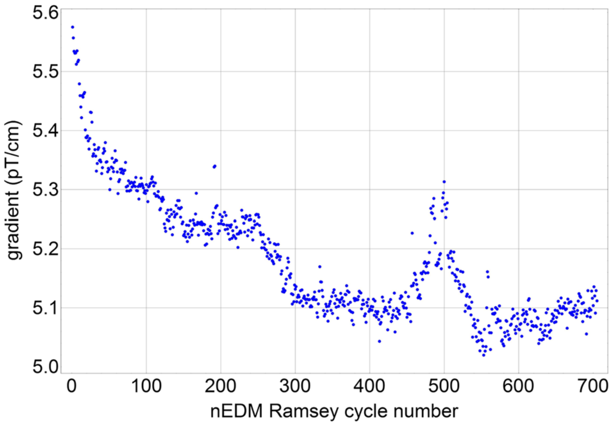

Fig. 6 Gradient evolution in one nEDM run i.e. in one configuration of magnetic field. 700 cycles correspond to 3 days of data taking

4.2 Gradient determination

The multipole expansion of the B_z components of the **B** field is used with the aim of obtaining $\partial B_z/\partial z$. The B_z component (approximately 1μT) of the **B** field is much larger than the transverse components B_x and B_y, which are typically below 10 nT, so we assume $|\mathbf{B}|$ = $B_z \gg B_x, B_y$. The expansion is used up to the second order (i.e. including dipole and quadrupole fields); this is determined by the number of available ^{133}Cs magnetometers. The B_z measured by a ^{133}Cs magnetometer at the position (x, y, z) is then expressed as

$$
\begin{aligned}
B_z(x, y, z) = & \; B_z + g_x x + g_y y + g_z z + g_{xx}(x^2 - z^2) \\
& + g_{yy}(y^2 - z^2) + g_{xy} xy \\
& + g_{xz} xz + g_{yz} yz \,,
\end{aligned} \tag{7}
$$

where the gradients are represented by e.g. $g_z = \partial B_z/\partial z$, and the nine parameters $(B_z, g_x, g_y, g_z, etc.)$ in front of the harmonic polynomials are obtained by solving a system of equations. This method is used to obtain the gradient value for each Ramsey cycle; the evolution of this gradient within a typical measurement run is shown in Fig. 6.

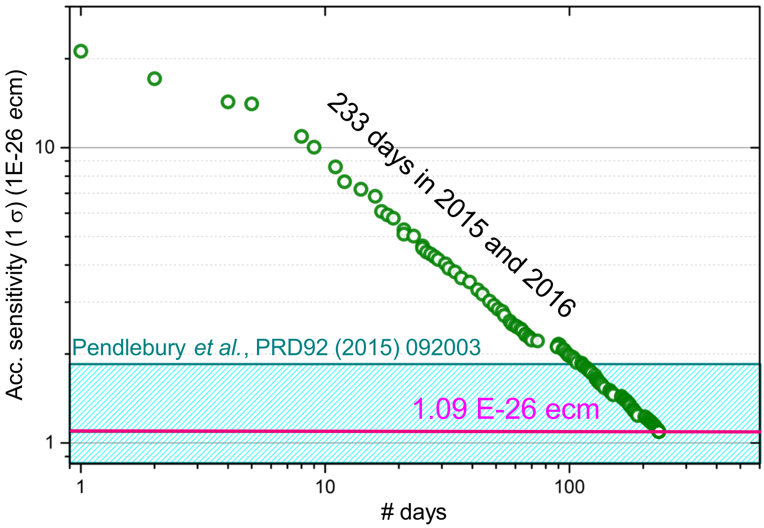

Fig. 7 The accumulated statistical sensitivity of the nEDM experiment before any cuts and selections

5 Conclusions

The nEDM experiment at PSI is currently taking data with the world's best statistical sensitivity of about 1.5×10^{-25} $e \cdot$ cm/day and has reached a cumulated uncertainty of $1.09 \times 10^{-26} e\cdot$cm as shown in Fig. 7 (as of September 2016). The cumulated statistical sensitivity at the end of 2016 is expected to be about $9 \times 10^{-27} e\cdot$cm which is at the similar level as the systematic effect contribution in the RAL/Sussex/ILL setup of $9.9 \times 10^{-27} e \cdot$cm as shown in table II of Ref. [12]. In the upgraded version of this setup at PSI the control of certain systematic effects, like for example the uncompensated magnetic field drift, has been improved which will reduce the systematic uncertainty by factor of about four. Further improvement of the statistical sensitivity is foreseen and will be realised by replacing the existing setup at PSI with a new apparatus with better adaptation to the UCN source and with a double precession chamber arrangement.

Acknowledgments The research presented in this article is a collaborative effort of all the members of the nEDM project and author would like to thank all the colleagues for the support. The collaborating institutions acknowledge the funding agencies.

References

1. Olive, K.A. et al.: (Particle Data Group). Chin. Phys. C **38**, 110 (2014)
2. Riotto, A.: Theories of Baryogenesis, arXiv:hep-ph/0907.2805 (1998)
3. Sakharov, A.D.: Violation of CP invariance, C asymmetry, and baryon asymmetry of the universe. Pisma Zh. Eksp. Teor. Fiz. **5**, 32 (1967)
4. Christenson, J.H., Cronin, J.W., Fitch, V.L., Turlay, A.: Evidence for the 2π decay of the K_2^0 meson. Phys. Rev. Lett. **13**, 138 (1964)
5. BABAR Collaboration: Observation of CP violation in the B0 meson system. Phys. Rev. Lett. **091801**, 87 (2001)

6. BELLE Collaboration: Observation of large CP violation in the neutral B meson system. Phys. Rev. Lett. **091802**, 87 (2001)
7. Nath, P. et al.: The hunt for new physics at the large hadron collider. Nucl. Phys. B **185**, 200–202 (2010)
8. King, S.F.: Models of neutrino mass, mixing and CP violation. J. Phys. G, Nucl. Part. Phys. **123001**, 42 (2015)
9. Engel, J., Ramsey-Musolf, M.-J., van Klock, U.: Electric dipole moments of nucleons, nuclei, and atoms: The standard model and beyond. Prog. Part. Nucl. Phys. **71**, 21 (2013)
10. Lueders, G.: Proof of the TCP theorem. Ann. Phys. **2**, 1 (1957)
11. Czarnecki, A., Marciano, W.: Electromagnetic Dipole Moments and New Physics. In: Roberts, B.L., Marciano, W.J. (eds.) Lepton Dipole Moments, World Scientific Publishing (2010)
12. Pendlebury, J.M., et al.: A revised experimental upper limit on the electric dipole moment of the neutron. Phys. Rev. D **092003**, 92 (2015)
13. Pospelov, M., Ritz, A.: Electric dipole moments as probes of new physics. Ann. Phys. **318**, 119 (2005)
14. Mohr, P.J., Taylor, B.N., Newell, D.B. The 2014 CODATA Recommended Values of the Fundamental Physical Constants (Web Version 7.1). This database was developed by J. Baker, M. Douma, and S. Kotochigova. Available: http://physics.nist.gov/constants [Sunday, 03-Jul-2016 04:03:16 EDT]. National Institute of Standards and Technology, Gaithersburg, MD 20899.
15. Afach, S. et al.: Dynamic stabilization of the magnetic field surrounding the neutron electric dipole moment spectrometer at the Paul Scherrer Insitute. J. Appl. Phys. **084510**, 116 (2014)
16. Baker, C.A. et al.: The search for the neutron electric dipole moment at the Paul Scherrer Institute. Phys. Proc. **17**, 159 (2011)
17. Lauss, B.: Startup of the high-intensity ultracold neutron source at the Paul Scherrer Institute. Hyperfine Interact. **212**, 21 (2012)
18. Baker, C.A. et al.: Apparatus for measurement of the electric dipole moment of the neutron using a cohabiting atomic-mercury magnetometer. Nucl. Inst. Meth. A **736**, 184 (2014)
19. Afach, S., et al.: A device for simultaneous spin analysis of ultracold neutrons. Eur. Phys. J. A **51**, 143 (2015)
20. Ban, G., et al. Ultracold neutron detection with ^6Li-doped glass scintilators, arXiv:1606.07432 [physics.ins-det]
21. Ramsey, N.F., A molecular beam resonance method with separated oscillating fields: Phys. Rev. **78**, 695 (1950)
22. Harris, P.G. The neutron EDM experiment, arXiv **0709**, 3100 (2007)
23. Green, K.: Performance of an atomic mercury magnetometer in the neutron EDM experiment. Nucl. Inst. Meth. A **404**, 381 (1998)
24. Groeger, S. et al.: A high-sensitivity laser-pumped Mx magnetometer. Eur. Phys. J. D **38**, 239 (2006)
25. Knowles, P., et al.: Laser-driven Cs magnetometer arrays for magnetic field measurement and control. Nucl. Inst. Meth. A **611**, 306 (2009)
26. Cagnac, B.: Ann. Phys. (Paris) **6**, 467 (1961)
27. Afach, S., et al.: A measurement of the neutron to ^{199}Hg magnetic moment ratio. Phys. Lett. B **739**, 128 (2014)
28. Afach, S., et al.: Measurements of a false electric dipole moment signal from ^{199}Hg atoms exposed to an inhomogeneous magnetic field. Eur. Phys. J. D **69**, 225 (2015)
29. Weis, A.: On the gyromagnetic ratio of the Cs atom Internal report (2011)
30. Castagna, N. et al.: A large sample study of spin relaxation and magnetometric sensitivity of paraffin-coated Cs vapor cells. Appl. Phys. B **96**, 763 (2009)